Flavokawain A inhibits high glucose-induced malignant progression of lung cancer cells by suppressing PRMT5-mediated PTEN neddylation and nuclear translocation

LEI ZHENG[1,2*], JUAN LI[3*], CHAO SONG[1,2], LEPING SHI[1,2], QIAN ZHOU[1,2] and YUYAO GUAN[1,2]

[1]Department of Pharmacy, Shandong Provincial Third Hospital, Shandong University, Jinan, Shandong 250013, P.R. China; [2]Shandong Provincial Key Medical and Health Discipline of Clinical Pharmacy, Shandong Provincial Third Hospital, Jinan, Shandong 250013, P.R. China; [3]Department of Pharmacy, The Second Qilu Hospital of Shandong University, Shandong University, Jinan, Shandong 250033, P.R. China

Received June 11, 2026; Accepted July 24, 2026

DOI: 10.3892/ol.2026.15818

Abstract. A high-glucose microenvironment is a key feature of tumor metabolic reprogramming that promotes lung cancer cell progression. Previous studies have revealed that protein arginine methyltransferase 5 (PRMT5) is overactivated in various cancers and regulates neddylation of the tumor suppressor phosphatase and tensin homolog (PTEN). This study established a high-glucose (25 mM) *in vitro* model using human non-small cell lung cancer A549 cells. Cell proliferation, invasion and cell cycle progression were assessed using the cell counting kit-8, Transwell, 5-ethynyl-2'-deoxyuridine and flow cytometry assays. The expression levels of neural precursor cells expressed developmentally downregulated protein 8 (NEDD8) and PTEN in total and nuclear protein fractions were analyzed using Western blotting and PTEN localization was determined using immunofluorescence. Cellular NEDD8 levels were manipulated by overexpressing Flag-NEDD8 and using MLN4924, an inhibitor of NEDD8-activating enzyme. The association between PTEN and NEDD8 was further assessed through co-immunoprecipitation. Finally, the mechanism underlying the action of flavokawain A (FKA) was explored by comparing its effects on high-glucose-induced PTEN neddylation with those of GSK3326595, a selective inhibitor of PRMT5. A high-glucose environment promoted A549 cell proliferation and viability while inhibiting cell apoptosis, accompanied by enhanced neddylation of PTEN and its nuclear translocation. NEDD8 overexpression promoted the nuclear import of PTEN; however, MLN4924 treatment effectively blocked this effect. FKA treatment markedly reduced PRMT5 activity, thereby reducing the neddylation modification of PTEN, limiting the nuclear localization of PTEN, ultimately inhibiting the proliferation and invasion ability of A549 cells and promoting cell apoptosis. Notably, GSK3326595 exhibited an inhibitory effect similar to that of FKA. The results indicated that FKA suppressed high glucose-induced carcinogenic effects by inhibiting PRMT5-mediated PTEN neddylation and subsequent nuclear translocation.

Correspondence to: Dr Qian Zhou or Dr Yuyao Guan, Department of Pharmacy, Shandong Provincial Third Hospital, Shandong University, 11 Wuyingshan Road, Jinan, Shandong 250013, P.R. China
E-mail: 202457070013@sdu.edu.cn
E-mail: guanxiaoyao0815@163.com

*Contributed equally

Abbreviations: CCK-8, Cell Counting Kit-8; Co-IP, co-immunoprecipitation; FKA, Flavokawain A; H3, Histone H3; IF, immunofluorescence; NEDD8, neural precursor cell expressed developmentally downregulated protein 8; NSCLC, non-small cell lung cancer; PRMT5, protein arginine methyltransferase 5; qPCR, quantitative PCR; SD, standard deviation; TME, tumor microenvironment; AAD, 7-aminoactinomycin D

Key words: flavokawain A, high glucose, phosphatase and tensin homolog, neddylation

Introduction

Lung cancer remains a leading cause of cancer mortality worldwide and non-small cell lung cancer (NSCLC) accounts for most lung cancer cases (1,2). Despite significant progress in targeted therapy and immunotherapy, the prognosis of patients with NSCLC remains poor (3). This poor outcome mainly reflects disease complexity, treatment resistance and the limited availability of meaningful molecular targets (4). Therefore, a deeper understanding of the pathways driving the occurrence and development of lung cancer and the identification of novel therapeutic targets is crucial to improve treatment and prognosis.

Recently, research has expanded from tumor-intrinsic features to the role of the tumor microenvironment (TME), including TME-driven metabolic reprogramming (5). Metabolic reprogramming has become a defining feature of cancer biology, distinguishing the metabolic phenotypes of cancer cells from normal cells in various tumor types (6). With the widespread increase in diabetes and obesity globally,

accumulating evidence indicates that high-glucose (HG) conditions are associated with increased cancer progression and worse prognosis, including reports in lung cancer (7-9). Chronic hyperglycemia provides excessive metabolic substrates for rapid tumor growth and serves as a powerful signaling factor that can remodel intracellular signaling and metabolic pathways (10). Glucose-mediated effects also involve the regulation of post-translational modifications of proteins, particularly neddylation, ultimately enhancing the proliferation, invasion and apoptosis resistance of cancer cells (11,12). Consequently, elucidating the molecular pathways through which a HG microenvironment reshapes the malignant phenotype of lung cancer cells has become a critical focus in tumor metabolism studies.

Phosphatase and tensin homolog (PTEN) is the most extensively studied tumor suppressor gene after p53. PTEN antagonizes the phosphatidylinositol-3-kinase/protein kinase B (PI3K/AKT) signaling pathway by dephosphorylating PIP3, thereby suppressing cell proliferation and promoting apoptosis (13). Under physiological conditions, PTEN shuttles between the cytoplasm and the nucleus. Cytoplasmic PTEN primarily inhibits PI3K/AKT signaling, whereas nuclear PTEN regulates DNA repair, chromosome stability and cell cycle progression (14). The function of PTEN is dependent on its subcellular localization. Abnormal nuclear PTEN accumulation may impair its classical tumor-suppressive functions and promote malignant progression (15,16).

Post-translational modifications are vital for regulating PTEN localization and function (17,18). Among these modifications, neddylation regulates the activity, stability and subcellular distribution of target proteins through the covalent attachment of neural precursor cell expressed developmentally downregulated protein 8 (NEDD8). PTEN undergoes neddylation, which facilitates its translocation from the cytoplasm to the nucleus (12). Excessive PTEN neddylation has been implicated in multiple tumor progression (19). However, whether a HG microenvironment induces abnormal PTEN nuclear translocation by altering neddylation remains unclear in lung cancer.

Flavokawain A (FKA) is a chalcone compound derived from *Piper methysticum* and exhibits multiple biological activities, including anti-inflammatory, antioxidant and anti-tumor effects (20). FKA inhibits the proliferation and invasion of various tumor cells and induces apoptosis and cell cycle arrest (21-23). Although its anti-cancer potential has been demonstrated whether FKA suppresses lung cancer progression by regulating PTEN neddylation and nuclear translocation under HG conditions remains unclear (24). Based on previous research results, it was proposed that FKA counteracts neddylation and subsequent nuclear accumulation of PTEN induced by high glucose levels, thereby suppressing HG-induced oncogenic phenotypes. To test this hypothesis, the present study established an *in vitro* HC model using A549 (human lung adenocarcinoma) cells, which were widely used in lung cancer research to investigate glucose-related tumor progression (25-27). The present study then investigated how elevated glucose levels affect cell proliferation, invasion, the molecular mechanisms regulating PTEN post-translational modification and subcellular localization. Subsequently, the present study evaluated whether FKA can specifically interrupt these glucose-driven changes, reduce PTEN neddylation, restore cytoplasmic localization and tumor suppressor function and ultimately reduce the malignant behavior of cancer cells. Through these studies, the present study aimed to elucidate the molecular pathways by which HG conditions promote lung cancer progression, clarify the FKA role in regulating PTEN function and localization under HG conditions and provide a basis for therapeutic strategy development against HG-related tumor development.

Materials and methods

Cell culture. A549 human lung adenocarcinoma cells (PromoCell; RRID: CVCL_0023l, contamination-free) were cultured in Ham's F-12K medium (PromoCell) supplemented with 10% fetal bovine serum (FBS; Gibco; Thermo Fisher Scientific, Inc.; cat. no. A5256701) and 1% penicillin-streptomycin (P/S; Dalian Meilun Biotechnology Co., Ltd.; cat. no. MA0110) and maintained at 37˚C in a humidified incubator with 5% carbon dioxide. Logarithmic-growth-phase cells were selected for the experiment. Prior to treatment, $2x10^5$ cells/well were seeded into plates and cultured until they reached 60% confluence. Subsequently, glucose starvation was induced by replacing the medium with a 5 mM glucose-containing medium. The cells were cultured for 24 h to deplete extracellular glucose. Following starvation, the cells were exposed to HG; 25 mM; MedChemExpress; cat. no. HY-13966) and cultured for an additional 24 h (28). In the FKA treatment group, cellular morphology was monitored daily using a light microscope (22).

Cell counting kit-8 (CCK-8) assay. A549 cells were seeded at $5x10^3$ cells/well in 96-well plates, with five technical replicates per group. Cell viability was assessed at 0, 24 and 48 h. Cell viability was expressed as the mean optical density (OD_{450}) value for each group.

Plasmid transfection. The cell density of A549 cells was 60-70% at the time of transfection. The plasmid (4 μg) and 6 μl Lipofectamine® 2000 (Invitrogen; Thermo Fisher Scientific, Inc.) were diluted separately with Opti-MEM to a final volume of 250 μl and incubated for 5 min at room temperature. The diluted Lipofectamine® 2000 (Invitrogen; Thermo Fisher Scientific, Inc.) was then mixed with the plasmid dilution and incubated at room temperature for 20 min. The transfection complexes were added to the cells and the culture medium was replaced 6 h after transfection. The cells were cultured for 48 h before the next experiment.

Transwell invasion assay. Briefly, 24-well Transwell chambers (8-μm pore size; Wuhan NEST Biotechnology Co., Ltd.) pre-coated with Matrigel at 37˚C for 30 min were used for the invasion assay. Starved or treated A549 cells were resuspended in serum-free medium and $2x10^4$ cells in 200 μl were seeded into the upper chamber. The lower chamber was filled with 600 μl complete medium containing 10% FBS (Gibco; Thermo Fisher Scientific, Inc.) to serve as the chemoattractant. After incubation at 37˚C for 24 h, non-invading cells

on the upper surface were removed using a cotton swab. The membranes were fixed with 4% paraformaldehyde for 15 min and stained with 0.1% crystal violet for 20 min at room temperature. Following PBS) washing and air-drying, invading cells were counted in five randomly selected fields under a light microscope.

Flow cytometric analysis. Processed cells were collected and washed twice with PBS. The cells were centrifuged at 1,000 x g for 3 min at 4˚C and the pellet was resuspended and fixed in pre-cooled 70% ethanol overnight at 4˚C. The cells were washed twice with PBS and resuspended in 500 μl of staining buffer containing propidium iodide (PI; 5 μg/ml) and RNase A (100 μg/ml). The cells were incubated in the dark at 37˚C for 30 min. For cell cycle analysis, ≥10,000 events were acquired using a flow cytometer and the data were analyzed to determine the distribution of cells in G_1, S and G_2/M phases. For apoptosis analysis, the cells were stained with Annexin V-PE and 7-AAD following the manufacturer's instructions (Annexin V-PE/7-AAD Apoptosis Detection Kit; Dalian Meilun Biotechnology Co., Ltd.; cat. no. MA0429) and analyzed within 1 h for detection by a flow cytometer (NovoCyte, Agilent Technologies) and analyzed with the built-in NoVo Express software. Cell apoptosis was calculated as early + late apoptosis rate.

Co-immunoprecipitation (Co-IP). Cells carrying Flag-Nedd8 or vector (Miaoling Plasmid Platform; cat. no. P73568) were collected and lysed in 500 μl radioimmunoprecipitation assay (RIPA, Cwbio, cat. no. CW2333S) buffer containing protease inhibitors (Servicebio, cat. no. G2007) for 30 min on the ice, followed by centrifugation at 11,500 g for 15 min at 4˚C to obtain the supernatant. Total protein (1 mg) was incubated with the indicated primary antibody, including anti-Flag (Proteintech Group, Inc.; cat. no. 80801-2-RR, 3 μg), or control IgG (Beyotime Biotechnology; cat. no. A7001, both 3 μg) under rotation at 4˚C overnight. Protein A/G magnetic beads (MedChemExpress; cat. no. HY-K0202; 30 μl) were then added and incubated for 2 h. After three washes with RIPA buffer containing protease inhibitors at 4˚C, the beads were resuspended in SDS loading buffer and heated at 95˚C for 5 min to denature the proteins. Western blotting was used to detect the expression of the related proteins.

Immunofluorescence staining (IF). Cells ($1x10^4$) were seeded into plates for experimental treatment. The cells were fixed with 4% paraformaldehyde for 15 min at room temperature, then permeabilized with 0.3% Triton X-100 for 10 min. After blocking with 5% bovine serum albumin (Servicebio; cat. no. G5001) for 1 h at room temperature, the cells were incubated with PTEN primary antibody (ABclonal Biotech Co., Ltd.; cat. no. A28510; 1:200) at 4˚C overnight. Following three washes with PBS, a secondary antibody (Abcam; cat. no. ab150077; 1:100) was added and incubated for 1 h at room temperature. Nuclei were counterstained with 4',6-Diamidino-2'-phenylindole (DAPI; Abcam; cat. no. ab104139) for 5 min at room temperature and after additional PBS washes, cells were mounted onto glass slides and images captured using a Nikon fluorescence microscope (magnification, x100).

Western blotting. Following lysis with RIPA (Cwbio, cat. no. CW2333S) buffer containing protease inhibitors (Servicebio, cat. no. G2007) for 30 min on the ice, total protein was extracted and quantified using the BCA assay. Briefly, 30 μg protein was separated by sodium dodecyl sulfate-polyacrylamide gel electrophoresis (15%) and transferred onto a PVDF membrane. The membranes were blocked with 5% skimmed milk for 1 h at 4˚C. Primary antibodies against NEDD8 (CST Biological Reagents Co., Ltd.; cat. no. 2745; 1:1,000), PTEN (ABclonal Biotech Co., Ltd.; cat. no. A28510, 1:1,000), histone H3 (H3; cat. no. 17168-1-AP, PTG; 1:10,000) and GAPDH (Proteintech Group, Inc.; cat. no. 60004-1-Ig, 1:10,000) were applied and incubated overnight at 4˚C. Following 0.05% Tween 20 (TBST) washing, membranes were incubated with horseradish peroxidase-conjugated goat anti-mouse IgG (H+L) or goat anti-rabbit IgG (H+L; Beijing Zhongshan Jinqiao Biotechnology Co., Ltd.; cat. no. ZB-2305 or ZB-2301; 1:10,000) for 1 h at room temperature. Signals were detected using enhanced chemiluminescence (Meilunbio, cat. no. MA0186-1) and band intensities were quantified using ImageJ software (National Institutes of Health, version 2.0.0).

Reverse transcription-quantitative (RT-q) PCR. In total, $5x10^5$ cells were collected and total RNA was isolated using TRIzol® (Invitrogen; Thermo Fisher Scientific, Inc. cat. no. 15596018CN) and its concentration and purity were determined spectrophotometrically. RNA was reverse-transcribed into cDNA using the Evo M-MLV RT Premix (Agbio, cat. no. AG11728) according to the manufacturer's instructions. qPCR was performed using the SYBR Green Premix Pro Taq HS qPCR Kit (Agbio, cat. no. AG11701). Thermocycling conditions were as follows: Initial denaturation (95˚C, 30s) was followed by 40 cycles of annealing (60˚C, 5s), extension (60˚C, 30s), and denaturation and a final cycle of annealing and prolonged extension. GAPDH served as the internal control and relative expression was calculated using the $2^{-\Delta\Delta Cq}$ method (29). These experiments were replicated 3 times and the primer sequences are presented in Table I.

EdU incorporation assay. Cell proliferation was detected using an EdU kit (Beyotime Biotechnology, cat. no. C0075S). Cells were seeded in 24-well plates for treatment. The EdU working solution (50 μM) was added and incubated at 37˚C for 2 h. Cells were fixed with 4% paraformaldehyde (Servicebio, cat. no. G1101) for 15 min and permeabilized with 0.5% Triton X-100 for 10 min at room temperature, followed by staining according to the manufacturer's protocol. The nuclei were counterstained with DAPI (10 mM solution in water) at room temperature and EdU-positive cells were imaged and quantified using a fluorescence microscope (Nikon Instruments Inc., cat. no. Eclipse Ts2-FL).

Nuclear and cytoplasmic protein extraction. The cells were harvested and washed twice with cold PBS. Cytoplasmic and nuclear fractions were isolated using the NE-PER Nuclear and Cytoplasmic Extraction Kit (Thermo Fisher Scientific, Inc.; cat. no. 78833) following the manufacturer's instructions. Briefly, the cells were resuspended in cytoplasmic extraction reagent I supplemented with protease inhibitors and incubated

Table I. Sequences of primers used for reverse transcription-quantitative PCR.

Gene	Forward primer (5'-3')	Reverse primer (5'-3')
NEDD8	AGACGCTGACCGGAAAGGA	TCATCATTCATCTGCTTGCCAC
GAPDH	AGAAGGCTGGGGCTCATTTG	AGGGGCCATCCACAGTCTTC

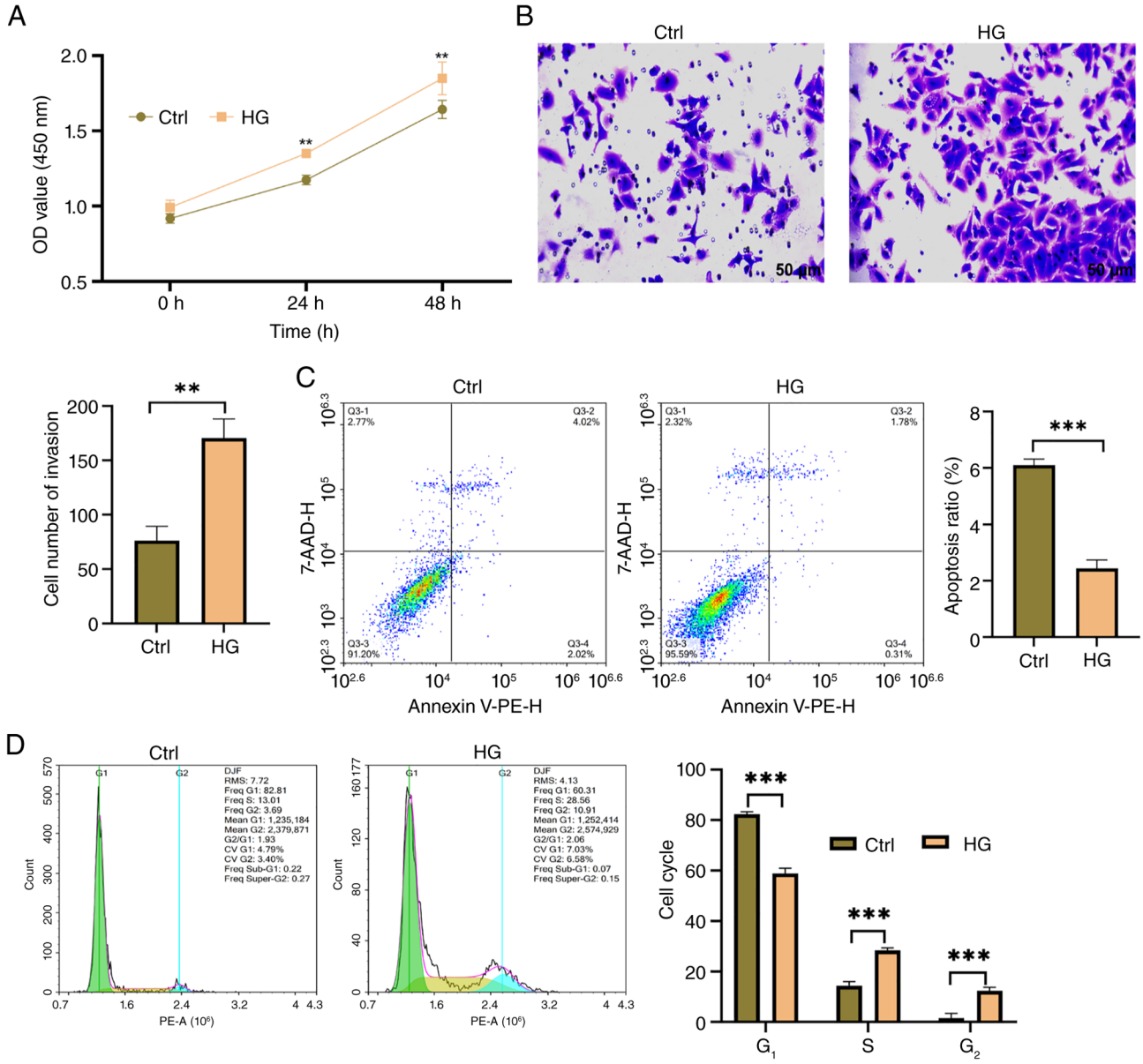

Figure 1. High glucose promotes the proliferation and invasion of A549 cells and inhibits apoptosis. (A) CCK-8 assay was performed to evaluate cell proliferation at 0, 24 and 48 h. (B) Transwell assay was used to determine cell invasion. Magnification, x200). (C) Flow cytometry following Annexin V/PI staining was conducted to quantify apoptosis. (D) Flow cytometry was used to analyze cell cycle distribution. All data are presented as the mean ± SD of three independent experiments. **P<0.01; ***P<0.001. OD, optical density; HG, high glucose; Ctrl, control.

on ice for 10 min. Cytoplasmic extraction reagent II was then added and samples were incubated on ice for 1 min before centrifugation at 16,000 x g for 5 min at 4˚C and the supernatant (cytoplasmic fraction) was collected. The nuclear pellet was resuspended in ice-cold nuclear extraction reagent (Thermo Fisher Scientific, Inc.) and incubated on ice for 40 min with vortexing every 10 min. Following centrifugation at 16,000 x g for 10 min at 4˚C, the supernatant (nuclear fraction) was collected. Protein concentrations were determined using a BCA assay. Histone H3 and GAPDH were used as nuclear and cytoplasmic markers, respectively.

Statistical analysis. All experiments were repeated at least thrice. Statistical analyses were performed using GraphPad

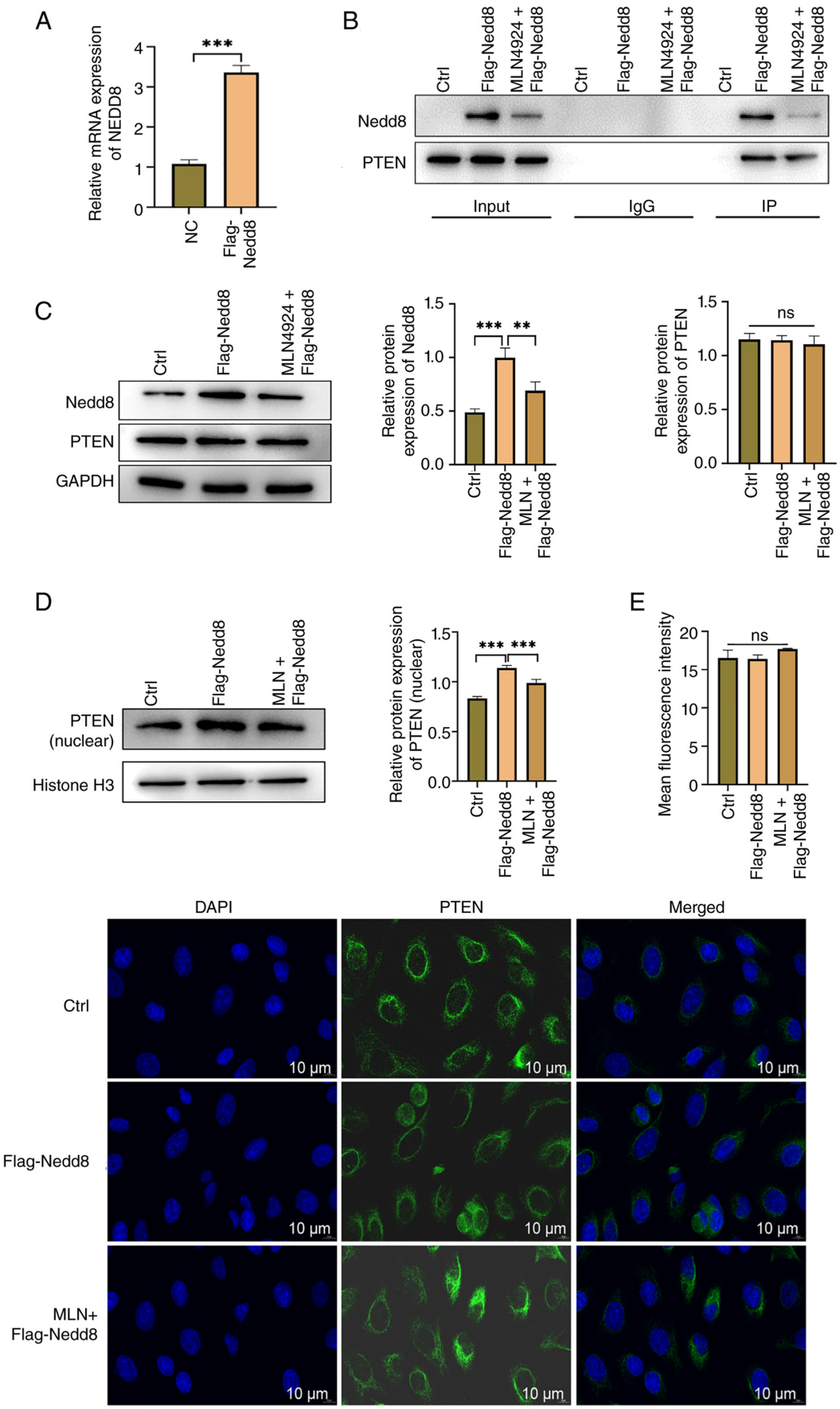

Figure 2. Neddylation promotes nuclear enrichment of PTEN under high glucose conditions. (A) Reverse transcription-quantitative PCR analysis of NEDD8 mRNA expression after Flag-NEDD8 overexpression. (B) Co-IP assay for the interaction between NEDD8 and PTEN. (C) Western blotting was conducted to detect the total protein levels of NEDD8, PTEN and (D) nuclear PTEN. (E) IF staining was conducted to visualize PTEN (green) and nuclei (DAPI, blue). Magnification, x800). **P<0.01; ***P<0.001. PTEN, phosphatase and tensin homolog; NEDD8, neural precursor cell expressed developmentally downregulated protein 8; Co-IP, co-immunoprecipitation; IF, immunofluorescence; DAPI, 4',6-diamidino-2-phenylindole; Ctrl, control.

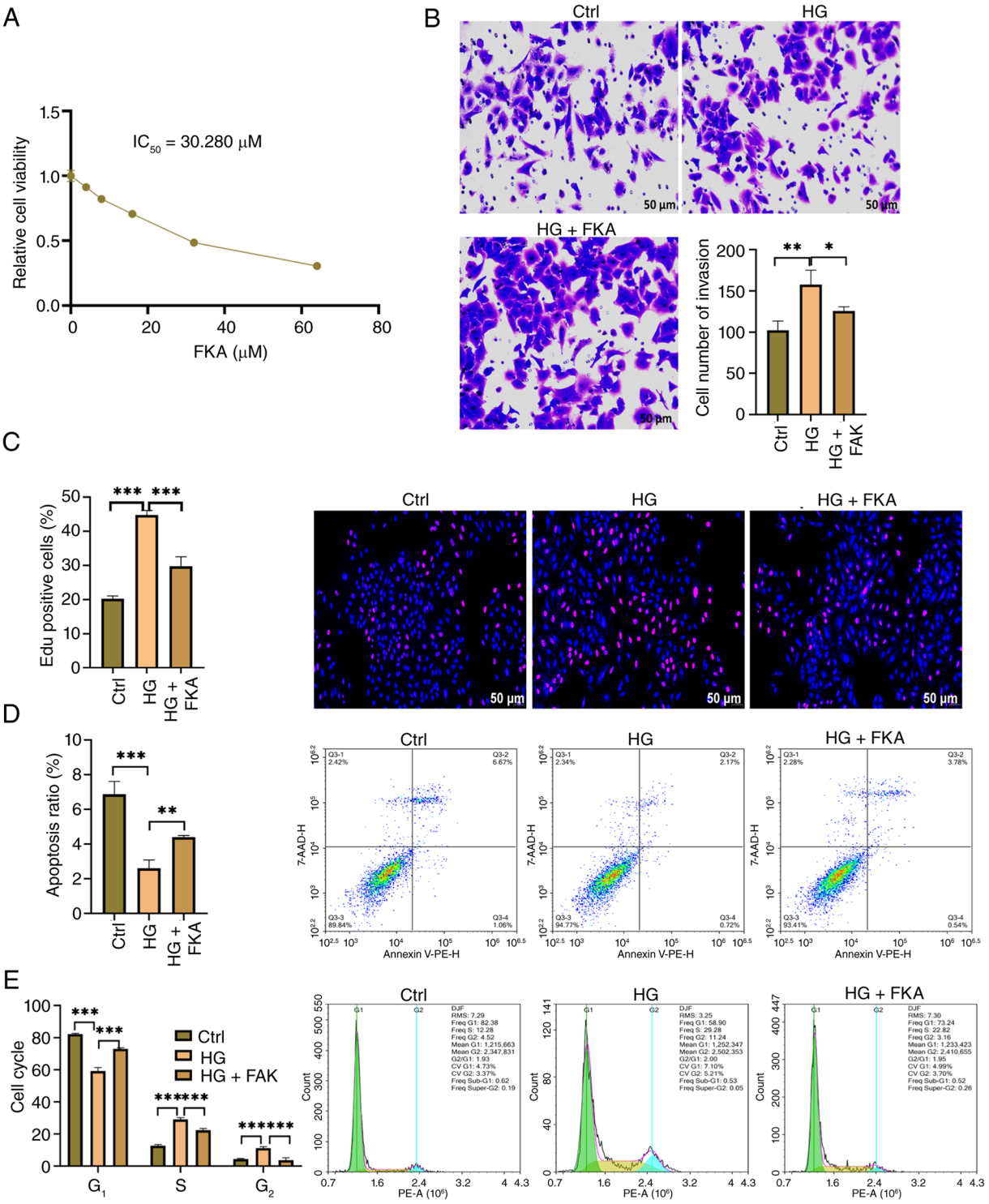

Figure 3. FKA inhibits the malignant phenotype of A549 cells induced by high glucose. (A) CCK-8 assays were used to determine cell viability. (B) Transwell assay was used to determine cell invasion (x200). (C) EdU assay was used to determine cell proliferation (x200). (D) Flow cytometry with Annexin V/PI staining was analyzed to determine the apoptotic rate. (E) Flow cytometry was used to analyze the cell cycle distribution. *P<0.05, **P<0.01 and ***P<0.001. FKA, flavokawain A; CCK-8, Cell Counting Kit-8; EdU, 5-ethynyl-2'-deoxyuridine; PI, propidium iodide; Ctrl, control.

Prism (GraphPad Prism 8; Dotmatics). Data are presented as mean ± standard deviation. Comparisons between two groups were performed using the independent sample t-test. Multiple groups were compared using one-way analysis of variance, followed by Tukey's test for pairwise comparisons between groups. P<0.05 was considered to indicate a statistically significant difference.

Results

HG promotes the proliferation and invasion of A549 cells and inhibits apoptosis. To study the effect of HG on lung adenocarcinoma A549 cells, the present study treated the cells with 25 mM glucose for 24 h and examined the resulting phenotypic changes. After 24 and 48 h of culture,

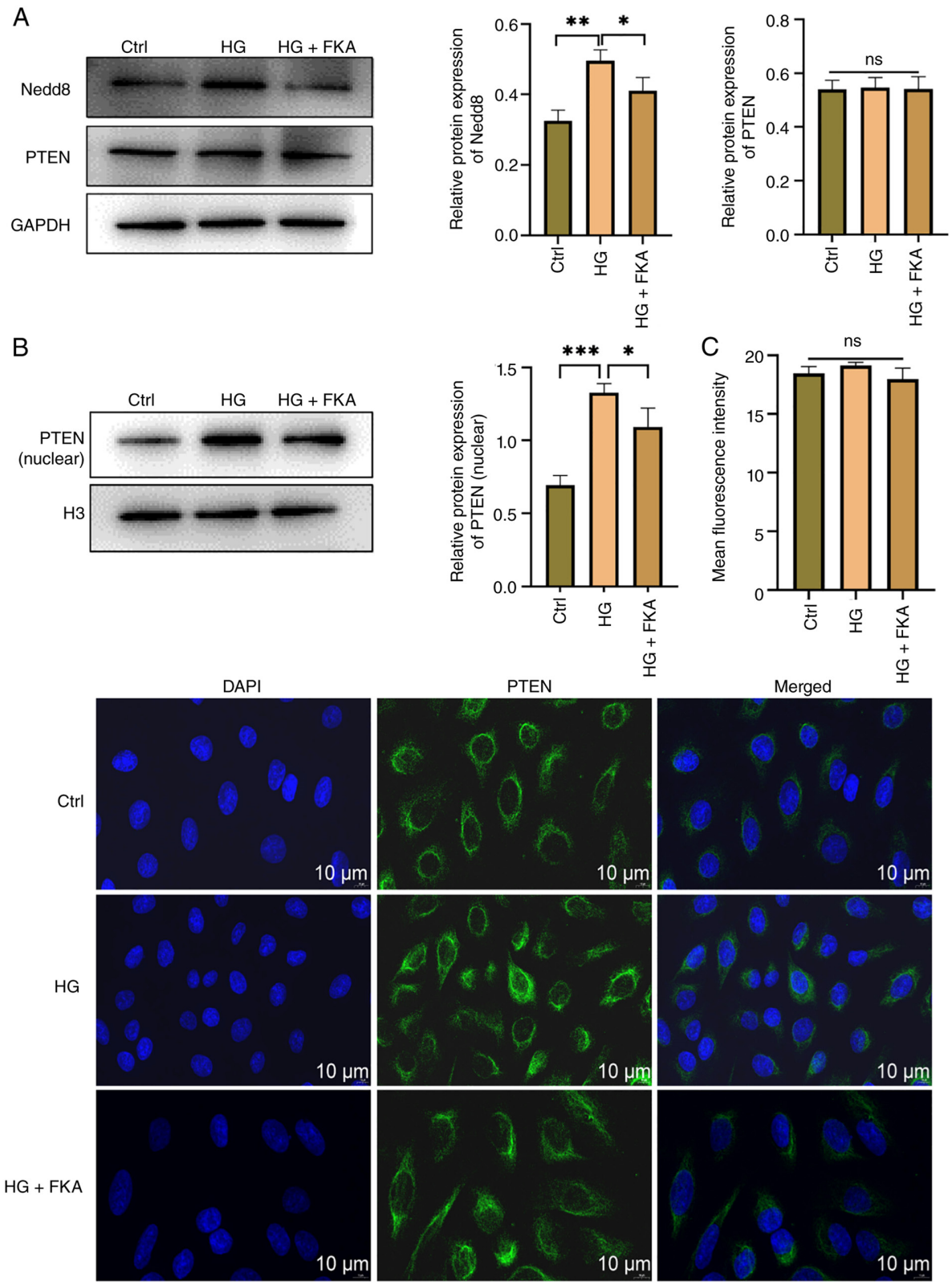

Figure 4. FKA reduces PTEN neddylation and nuclear enrichment caused by high glucose. (A) Western blotting was conducted to detect the total protein levels of NEDD8 and PTEN. (B) Western blotting was conducted to detect the total protein levels of nuclear PTEN. (C) IF staining was conducted to visualize PTEN (green) and nuclei (DAPI, blue) (x800). All data are presented as mean ± SD of three independent experiments. *P<0.05; **P<0.01; ***P<0.001. FKA, flavokawain A; PTEN, phosphatase and tensin homolog; NEDD8, neural precursor cell expressed developmentally downregulated protein 8; ns, not significant; IF, immunofluorescence; DAPI, 4',6-diamidino-2-phenylindole; HG, high glucose; Ctrl, control.

cell viability in the HG group was markedly higher than that in the control group (Fig. 1A). Compared with the control group, the number of migrating cells markedly increased following HG treatment (Fig. 1B) and the overall apoptosis in the HG group was markedly reduced (Fig. 1C). HG decreased the G_1-phase cell proportion and increased S- and G_2-phase

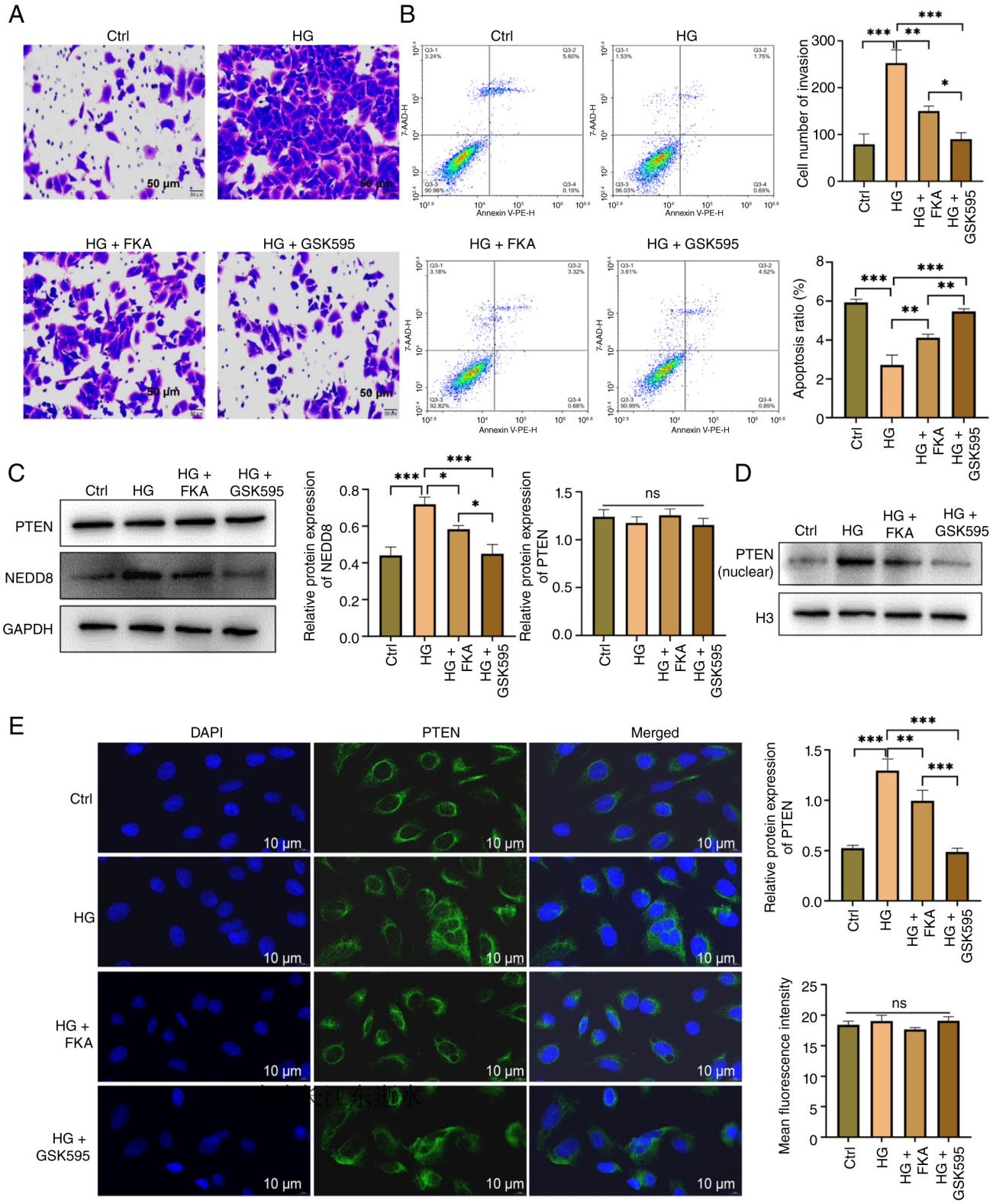

Figure 5. FKA regulates PTEN neddylation via PRMT5 to inhibit the pro-cancer effect of high glucose. (A) Transwell assay was used to determine cell invasion (x200). (B) Flow cytometry with Annexin V/PI staining was analyzed to determine the apoptotic rate. (C) Western blotting was conducted to detect the total protein levels of NEDD8, PTEN and (D) nuclear PTEN. (E) IF was conducted to visualize PTEN (green) and nuclei (DAPI, blue) (x800). All data are presented as the mean ± SD of three independent experiments. *P<0.05; **P<0.01; ***P<0.001. ns, not significant; FKA, flavokawain A; PTEN, phosphatase and tensin homolog; PRMT5, protein arginine methyltransferase 5; PI, propidium iodide; NEDD8, neural precursor cell expressed developmentally downregulated protein 8; IF, immunofluorescence; DAPI, 4',6-diamidino-2-phenylindole; HG, high glucose; Ctrl, control.

cell proportions (Fig. 1D). In conclusion, a HG microenvironment accelerates cell-cycle progression in A549 cells and exerts pro-proliferative, pro-migratory and anti-apoptotic effects, indicating a typical pro-tumorigenic phenotype.

Neddylation promotes the nuclear enrichment of PTEN under HG conditions. To determine whether the HG-induced pro-tumorigenic effect was associated with PTEN neddylation and nuclear translocation and given that NEDD8 is central to neddylation (30), the present study overexpressed Flag-NEDD8 in A549 cells (Fig. 2A). The present study subsequently performed Co-IP assays to examine the interaction between Flag-NEDD8 and PTEN. Co-IP results revealed that Flag-NEDD8 interacted with PTEN (Fig. 2B), suggesting that PTEN may undergo neddylation. Although total PTEN levels remained unchanged after HG treatment and Flag-NEDD8 overexpression, nuclear PTEN levels markedly increased and this enrichment was reduced by MLN4924 treatment (Fig. 2C-E). In summary, HG and NEDD8 overexpression promote nuclear PTEN enrichment. However, MLN4924 blocks this effect, indicating that NEDD8-mediated neddylation is a key mechanism driving PTEN nuclear translocation under HG conditions.

FKA inhibits the malignant phenotype of A549 cells induced by HG. The initial experiments of the present study verified the tumor-promoting effects of hyperglycemia. Prior to examining the biological actions of FKA in detail, the present study evaluated its influence on the viability of A549 cells exposed to HG and determined that 30 μM represented an appropriate working concentration for subsequent studies (Fig. 3A). FKA markedly reversed the HG-induced pro-tumorigenic phenotype. It markedly inhibited HG-enhanced cell invasion and reduced cell proliferation (Fig. 3B-C). FKA also markedly increased apoptosis under HG conditions (Fig. 3D). Cell cycle analysis exhibited that FKA reversed the HG-induced reduction in G_1-phase cells and restored S- and G_2-phase cell proportions (Fig. 3E). In conclusion, FKA effectively suppresses the HG-driven malignant phenotype of A549 cells. Although it did not completely restore all parameters to normal glucose levels, the observed effects were statistically significant across all assays.

FKA reduces PTEN neddylation and nuclear enrichment caused by HG. To clarify how FKA reverses the HG-induced pro-tumorigenic effect, the present study examined its effects on PTEN localization and modification. Molecular analysis revealed that FKA markedly reduced nuclear PTEN under HG and decreased total NEDD8 expression and PTEN neddylation induced by HG (Fig. 4A). FKA also markedly decreased the nuclear localization of PTEN (Fig. 4B-C). Consequently, FKA blocks abnormal PTEN localization by reducing HG-induced PTEN neddylation and nuclear enrichment.

FKA regulates PTEN neddylation via PRMT5 to inhibit the pro-cancer effect of HG. Given that FKA inhibits PRMT5 activity (31), the present study examined whether PRMT5 participates in FKA-mediated regulation of PTEN neddylation. In functional assays, the PRMT5 inhibitor GSK3326595 revealed effects similar to FKA, markedly reducing HG-induced cell proliferation and invasion (Fig. 5A) and promoting apoptosis (Fig. 5B). Mechanistic studies indicated that FKA and GSK3326595 markedly reduced HG-induced NEDD8 and nuclear PTEN levels (Fig. 5C-D) and decreased PTEN nuclear localization (Fig. 5E). Overall, PRMT5 inhibitor and FKA exhibit consistent functional and molecular effects, supporting PRMT5 as a key target of FKA. FKA may inhibit the HG-driven pro-tumorigenic process by suppressing PRMT5 activity and decreasing PTEN neddylation.

Discussion

Consistent with previous studies demonstrating that HG promotes tumor cell proliferation and migration in lung adenocarcinoma (7,25,26), the present study further extended these observations by revealing a novel mechanism involving PTEN neddylation and nuclear translocation. HG markedly enhanced cell cycle progression, thereby promoting proliferation and suggesting that certain cell cycle checkpoints may be bypassed under HG conditions. The HG-induced pro-tumorigenic phenotype was mediated by enhanced growth factor signaling and a neddylation-related mechanism that alters the localization of tumor suppressors, including PTEN, thereby weakening their molecular inhibitory effects on tumor growth. Previous reports have indicated that cancer incidence and mortality are higher in patients with diabetes (32,33). This suggests that metabolic dysregulation may contribute to tumor initiation and progression. HG promote tumor cell growth by activating the insulin/IGF-1 axis and downstream PI3K/AKT/mTOR pathway (13,34). However, the present study extended these findings by associating the HG-induced malignant phenotype with the abnormal subcellular localization of the tumor suppressor PTEN.

PTEN is a key lipid and protein phosphatase and its loss of function or decreased activity is a hallmark of numerous types of cancer (35,36). Although PTEN predominantly functions in the cytoplasm by dephosphorylating PI(3,4,5)P3 to antagonize the PI3K/AKT pathway, nuclear PTEN also has independent tumor-suppressive functions (37,38). Nuclear PTEN helps maintain genomic stability and regulates the cell cycle by interacting with chromatin and DNA damage repair proteins (39). HG and NEDD8 overexpression together led to marked nuclear enrichment of PTEN, which could be blocked by the neddylation inhibitor MLN4924 (40). This suggested that neddylation is a key driver of PTEN nuclear translocation under HG conditions. Although nuclear translocation of PTEN increases its nuclear abundance, it may reduce its ability to inhibit AKT signaling in the cytoplasm (41,42). Moreover, post-translational modifications, including ubiquitination and phosphorylation, influence PTEN localization and neddylation, which is structurally similar to ubiquitination, also regulates the stability or localization of substrates, including HIF-1α (43,44). The present study added a new link to PTEN regulation, revealing that HG drive neddylation-mediated PTEN mislocalization, placing it in a subfunctional state that weakens its tumor-suppressive activity and facilitates malignant cell proliferation. After PTEN enters the nucleus, its accumulation is accompanied by functional alterations. Under normal circumstances, nuclear PTEN helps maintain genomic stability. However, under HG conditions, PTEN undergoes neddylation, impairing its tumor-suppressive function in the nucleus. HG affect PTEN activity in the cytoplasm and nucleus, reduce the overall tumor suppressor ability and promote the malignant progression of lung cancer cells.

PRMT5, a key arginine methyltransferase, promotes tumor progression by regulating the expression of proteins associated with the cell cycle, RNA splicing and DNA repair (45). The present study further explored the molecular mechanism by which HG regulates the intracellular distribution of PTEN via neddylation. The results revealed that after treating cells with the PRMT5 inhibitor GSK3326595, its biological effects resemble the effects of FKA (46); both can inhibit cell proliferation and invasion induced by HG and promote cell apoptosis. Molecular analysis indicated that both drugs downregulated the expression level of NEDD8 and reduced the nuclear accumulation of PTEN caused by HG.

The present study suggested that PRMT5 functions upstream of PTEN neddylation-regulatory network. PRMT5 likely regulates the modification and localization of PTEN by influencing the expression or activity of key enzymes (including E1, E2 and E3) in neddylation or by regulating NEDD8 stability (47). Previous studies have revealed that PRMT5 regulates the activity of the E3 ligase Mouse double minute 2 homolog, supporting its potential role in regulating other E3 ligases (48). Cullin4A (CUL4A) and DDB1-CUL4-NEDD8 complex in the neddylation pathway has been reported, suggesting a possible involvement in this process (49). HG enhances the neddylation of key proteins and activates PRMT5, promoting PTEN nuclear translocation, providing a new theoretical perspective for metabolic changes promoting the occurrence and development of lung cancer.

Functional assays revealed that FKA effectively counteracts the malignant changes caused by HG, inhibiting invasion and proliferation and promoting apoptosis. The effect of FKA resembled that of GSK3326595. Additionally, FKA reduced the neddylation and nuclear accumulation of PTEN. These results supported the hypothesis that FKA regulates this pathway by influencing PRMT5. Accordingly, FKA could be a potential therapeutic agent for metabolic disorder-associated lung cancer, particularly for patients with hyperglycemia or diabetes. Notably, FKA suppresses HG-induced oncogenic signaling and inhibits the tumor-promoting effect of PRMT5. Although FKA is derived from natural products and has a complex structure, which could complicate drug development, its clear mechanism provides a rationale for developing FKA derivatives or novel therapeutic strategies for hyperglycemia-associated lung cancer. Notably, while FKA markedly counteracted the malignant changes caused by HG, the reversal was incomplete. This partial effect may reflect several factors: i) FKA primarily targets the PRMT5-PTEN neddylation pathway, but HG may promote tumor progression through additional parallel pathways (for example, RAGE-NOX-ROS signaling and PI3K/AKT/mTOR activation); ii) the 30 μM concentration represents an optimized dose that balances efficacy and cytotoxicity; iii) FKA, as a natural product, may have multiple cellular targets beyond PRMT5. Future studies combining FKA with other agents targeting complementary pathways may achieve a more complete inhibition of HG-induced tumor progression. Although FKA exhibits promising anti-cancer effects, its safety profile warrants careful consideration, particularly regarding hepatotoxicity. Li *et al* (27) demonstrated that dietary feeding of FKA for 3 weeks revealed no adverse effects on liver function in mice, with normal serum ALT and AST levels and normal liver histology.

Furthermore, Pinner *et al* (50) reported that FKA (≤100 μM) is not toxic to HepG2 hepatocytes and activated protective heat shock and antioxidant responses via nuclear factor erythroid 2-related factor 2 and heat shock factor protein 1 pathways, suggesting potential cytoprotective effects. Conversely, it is reported that FKA or flavokawain B could markedly enhance acetaminophen-induced hepatotoxicity in C57BL/6 mice even if they are safe when given alone, demonstrating herb-drug interaction risks (51). Similarly, kava hepatotoxicity cases in humans have been associated with concomitant medication use, suggesting that FKA's hepatotoxic potential may be context-dependent rather than inherent (52).

In conclusion, the present study provided new insights into how chronic HG accelerates NSCLC development. HG activated PRMT5, inducing abnormal neddylation and nuclear localization of PTEN, which weakens its tumor-suppressive function. Together, the findings indicated that FKA can prevent this process, thereby reversing the carcinogenic changes induced by HG. Future studies are required to verify the *in vivo* effects of FKA in animal models and assess its safety. Moreover, further studies are needed to elucidate the specific regulatory mechanism of PRMT5 in neddylation, including whether it directly regulates the E3 enzyme responsible for PTEN modification.

In summary, a HG environment can induce abnormal modifications and nuclear translocation of PTEN, thereby weakening its tumor suppressor function and promoting the proliferation and invasion of A549 cells. FKA can inhibit PRMT5 activation, prevent PTEN neddylation and nuclear translocation, reduce neddylation and nuclear accumulation of PTEN and thereby suppress the HG-induced malignant phenotype.

Acknowledgements

Not applicable.

Funding

The present study was supported by Shandong Provincial Natural Science Foundation (grant nos. ZR2022MH250, ZR2023MH150, ZR2025MS1281, ZR2025LSW046 and ZR2025QC2261Z), 2021 Shandong Medical Association Clinical Research Fund-Qilu Special Project (grant no. YXH2022ZX02050), Talent Program of Shandong Provincial Third Hospital (grant nos. jqrc008 and jqrc003), Shandong Province Medical and Health Technology Project (grant nos. 202313010259 and 202413050441) and Project of Shandong Provincial Health and Medical Management Research Center (grant no. SDWJYJ2025CB006).

Availability of data and material

The data generated in the present study are included in the figures and/or tables of this article.

Authors' contributions

LZ was responsible for conceptualization, formal analysis, funding acquisition, writing the original draft, and writing, reviewing and editing. JL and CS analyzed data, and wrote and

edited the manuscript. YG and LS were responsible for formal analysis, methodology, writing, reviewing and editing. QZ was responsible for conceptualization, writing the original draft, and writing, reviewing and editing. LZ and QZ confirm the authenticity of all the raw data. All authors read and approved the final manuscript.

Ethics approval and consent to participate

Not applicable.

Patient consent for publication

Not applicable.

Competing interests

The authors declare that they have no competing interests.

References

1. Cords L, Engler S, Haberecker M, Rüschoff JH, Moch H, de Souza N and Bodenmiller B: Cancer-associated fibroblast phenotypes are associated with patient outcome in non-small cell lung cancer. Cancer Cell 42: 396-412.e5, 2024.
2. Haratake N, Ozawa H, Morimoto Y, Yamashita N, Daimon T, Bhattacharya A, Wang K, Nakashoji A, Isozaki H, Shimokawa M, *et al*: MUC1-C is a common driver of acquired osimertinib resistance in NSCLC. J Thorac Oncol 19: 434-450, 2024.
3. Meyer ML, Fitzgerald BG, Paz-Ares L, Cappuzzo F, Jänne PA, Peters S and Hirsch FR: New promises and challenges in the treatment of advanced non-small-cell lung cancer. Lancet 404: 803-822, 2024.
4. Landre T, Assié JB, Chouahnia K, Des Guetz G, Auliac JB and Chouaïd C: First-line concomitant EGFR-TKI + chemotherapy versus EGFR-TKI alone for advanced EGFR-mutated NSCLC: A meta-analysis of randomized phase III trials. Expert Rev Anticancer Ther 24: 775-780, 2024.
5. Dey P, Kimmelman AC and DePinho RA: Metabolic codependencies in the tumor microenvironment. Cancer Discov 11: 1067-1081, 2021.
6. Nicolini A and Ferrari P: Involvement of tumor immune microenvironment metabolic reprogramming in colorectal cancer progression, immune escape, and response to immunotherapy. Front Immunol 15: 1353787, 2024.
7. Cai L, Hammond NG, Tasdogan A, Alsamraae M, Yang C, Cameron RB, Quan P, Solmonson A, Gu W, Pachnis P, *et al*: High glucose contribution to the TCA cycle is a feature of aggressive Non-Small cell lung cancer in patients. Cancer Discov 15: 702-716, 2025.
8. Supabphol S, Seubwai W, Wongkham S and Saengboonmee C: High glucose: An emerging association between diabetes mellitus and cancer progression. J Mol Med (Berl) 99: 1175-1193, 2021.
9. Watson MJ, Vignali PDA, Mullett SJ, Overacre-Delgoffe AE, Peralta RM, Grebinoski S, Menk AV, Rittenhouse NL, DePeaux K, Whetstone RD, *et al*: Metabolic support of tumour-infiltrating regulatory T cells by lactic acid. Nature 591: 645-651, 2021.
10. Vaziri-Gohar A, Hue JJ, Abbas A, Graor HJ, Hajihassani O, Zarei M, Titomihelakis G, Feczko J, Rathore M, Chelstowska S, *et al*: Increased glucose availability sensitizes pancreatic cancer to chemotherapy. Nat Commun 14: 3823, 2023.
11. Du MG, Peng ZQ, Gai WB, Liu F, Liu W, Chen YJ, Li HC, Zhang X, Liu CH, Zhang LQ, *et al*: The absence of PTEN in breast cancer is a driver of MLN4924 resistance. Front Cell Dev Biol 9: 667435, 2021.
12. Xie P, Peng Z, Chen Y, Li H, Du M, Tan Y, Zhang X, Lu Z, Cui CP, Liu CH, *et al*: Neddylation of PTEN regulates its nuclear import and promotes tumor development. Cell Res 31: 291-311, 2021.
13. Li F, Wan X, Li Z and Zhou L: High glucose inhibits autophagy and promotes the proliferation and metastasis of colorectal cancer through the PI3K/AKT/mTOR pathway. Cancer Med 13: e7382, 2024.
14. Liu F, Liu W, Tan Y, Shang Y, Ling S, Jiang X, Zhang Z, Sun S and Xie P: PTEN neddylation aggravates CDK4/6 inhibitor resistance in breast cancer. Oncogene 44: 2997-3013, 2025.
15. Ferdosi SR, Taylor B, Lee M, Tang N, Peng S, Bybee R, Reid G, Hartman L, Garcia-Mansfield K, Sharma R, *et al*: PTEN loss drives resistance to the neddylation inhibitor MLN4924 in glioblastoma and can be overcome with TOP2A inhibitors. Neuro Oncol 24: 1857-1868, 2022.
16. Taylor B, Tang N, Hao Y, Lee M, Peng S, Bybee R, Hartman L, Garcia-Mansfield K, Sharma R, Pirrotte P, *et al*: Glioblastoma vulnerability to neddylation inhibition is dependent on PTEN status, and dysregulation of the cell cycle and DNA replication. Neuro-oncology advances 6: vdae104, 2024.
17. González-García A, Garrido A and Carrera AC: Targeting PTEN regulation by post translational modifications. Cancers (Basel) 14: 5613, 2022.
18. Howitt J, Lackovic J, Low LH, Naguib A, Macintyre A, Goh CP, Callaway JK, Hammond V, Thomas T, Dixon M, *et al*: Ndfip1 regulates nuclear Pten import in vivo to promote neuronal survival following cerebral ischemia. J Cell Biol 196: 29-36, 2012.
19. Goenka A and Cheng SY: Targeting neddylation in cancer. Neuro Oncol 24: 1869-1870, 2022.
20. Song L, Mino M, Yamak J, Nguyen V, Lopez D, Pham V, Fazelpour A, Le V, Fu D, Tippin M, *et al*: Flavokawain A reduces Tumor-initiating properties and stemness of prostate cancer. Front Oncol 12: 943846, 2022.
21. Wang K, Zhang W, Wang Z, Gao M, Wang X, Han W, Zhang N and Xu X: Flavokawain A inhibits prostate cancer cells by inducing cell cycle arrest and cell apoptosis and regulating the glutamine metabolism pathway. J Pharm Biomed Anal 186: 113288, 2020.
22. Gayen S, Roy S, Laishram D, Bandyopadhyay SN and Mukherjee S: Flavokawain A Ruthenium-p-cymene complex-induced apoptosis by the modulation of PI3K/β-catenin/HER2/PARP signalling in lung cancer. Clin Exp Pharmacol Physiol 52: e70030, 2025.
23. Jandial DD, Krill LS, Chen L, Wu C, Ke Y, Xie J, Hoang BH and Zi X: Induction of G2M arrest by flavokawain A, a kava chalcone, increases the responsiveness of HER2-Overexpressing breast cancer cells to herceptin. Molecules 22: 462, 2017.
24. Zhang M, Xue J, Chen X, Elsaid FG, Salem ET, Ghanem RA, El-Kott AF and Xu Z: Bioactivity of hamamelitannin, flavokawain A, and triacetyl resveratrol as natural compounds: Molecular docking study, anticolon cancer, and anti-Alzheimer potentials. Biotechnol Appl Biochem 70: 730-745, 2023.
25. Liao YF, Yin S, Chen ZQ, Li F and Zhao B: High glucose promotes tumor cell proliferation and migration in lung adenocarcinoma via the RAGE-NOXs pathway. Molecular medicine reports 17: 8536-8541, 2018.
26. Sorin S, Zhou Y, Thithuan K, Khawkhiaw K, Zeng F, Ruangpratyakul T, Chomphoo S, Seubwai W, Wongkham S and Saengboonmee C: High glucose enhances the aggressiveness of lung adenocarcinoma via activating epidermal growth factor receptor/signal transducer and activator of transcription 3 pathways. J Nutr Biochem 119: 109399, 2023.
27. Li X, Xu X, Ji T, Liu Z, Gu M, Hoang BH and Zi X: Dietary feeding of Flavokawain A, a Kava chalcone, exhibits a satisfactory safety profile and its association with enhancement of phase II enzymes in mice. Toxicol Rep 1: 2-11, 2014.
28. Mao X, Huang L, Liu X, Lin X, Wu Q, Wang X, Ren Y, Ma J, Zhang M, Lin Y, *et al*: High glucose levels promote glycolysis and cholesterol synthesis via ERRα and suppress the autophagy-lysosomal pathway in endometrial cancer. Cell Death Dis 16: 182, 2025.
29. Livak KJ and Schmittgen TD: Analysis of relative gene expression data using real-time quantitative PCR and the 2(-Delta Delta C(T)) method. Methods 25: 402-408, 2001.
30. Yu M, Qian X, Wang Y, Li Q, Peng C, Chen B, Fang P, Shang W and Zhang Z: Emerging role of NEDD8-mediated neddylation in age-related metabolic diseases. Ageing Res Rev 94: 102191, 2024.
31. Liu S, Liu Z, Piao C, Zhang Z, Kong C, Yin L and Liu X: Flavokawain A is a natural inhibitor of PRMT5 in bladder cancer. J Exp Clin Cancer Res 41: 293, 2022.
32. Harborg S, Kjærgaard KA, Thomsen RW, Borgquist S, Cronin-Fenton D and Hjorth CF: New horizons: Epidemiology of obesity, diabetes mellitus, and cancer prognosis. J Clin Endocrinol Metab 109: 924-935, 2024.

33. Sirtori CR, Castiglione S and Pavanello C: Metformin: From diabetes to cancer to prolongation of life. Pharmacol Res 208: 107367, 2024.
34. Moreau F, Kirk NS, Zhang F, Gelfanov V, List EO, Chrudinová M, Venugopal H, Lawrence MC, Jimenez V, Bosch F, *et al*: Interaction of a viral insulin-like peptide with the IGF-1 receptor produces a natural antagonist. Nat Commun 13: 6700, 2022.
35. Exposito F, Redrado M, Houry M, Hastings K, Molero-Abraham M, Lozano T, Solorzano JL, Sanz-Ortega J, Adradas V, Amat R, *et al*: PTEN loss confers resistance to Anti-PD-1 therapy in Non-Small cell lung cancer by increasing tumor infiltration of regulatory T cells. Cancer Res 83: 2513-2526, 2023.
36. Zhang B, Liu M, Mai F, Li X, Wang W, Huang Q, Du X, Ding W, Li Y, Barwick BG, *et al*: Interruption of KLF5 acetylation promotes PTEN-deficient prostate cancer progression by reprogramming cancer-associated fibroblasts. J Clin Invest 134: e175949, 2024.
37. Azzi A: SHIP2 inhibition alters redox-induced PI3K/AKT and MAP kinase pathways via PTEN over-activation in cervical cancer cells. FEBS Open Bio 10: 2191-2205, 2020.
38. Naderali E, Khaki AA, Rad JS, Ali-Hemmati A, Rahmati M and Charoudeh HN: Regulation and modulation of PTEN activity. Mol Biol Rep 45: 2869-2881, 2018.
39. Sharma A and Almasan A: Autophagy and PTEN in DNA damage-induced senescence. Adv Cancer Res 150: 249-284, 2021.
40. Gu S, Lin C, Li Y, Wei Z, Cao B, Shen Z and Deng H: Neddylation inhibitor MLN4924 sensitizes head and neck squamous carcinoma cells to (S)-10-hydroxycamptothecin. Eur J Med Res 28: 326, 2023.
41. Guo Y, He J, Zhang H, Chen R, Li L, Liu X, Huang C, Qiang Z, Zhou Z, Wang Y, *et al*: Linear ubiquitination of PTEN impairs its function to promote prostate cancer progression. Oncogene 41: 4877-4892, 2022.
42. Wang Y, Liu J, Akatsu C, Zhang R, Zhang H, Zhu H, Liu K, Zhu HY, Min Q, Meng X, *et al*: LAPTM5 mediates immature B cell apoptosis and B cell tolerance by regulating the WWP2-PTEN-AKT pathway. Proc Natl Acad Sci USA 119: e2205629119, 2022.
43. Rashid M, Zadeh LR, Baradaran B, Molavi O, Ghesmati Z, Sabzichi M and Ramezani F: Up-down regulation of HIF-1α in cancer progression. Gene 798: 145796, 2021.
44. Yang Z, Su W, Wei X, Pan Y, Xing M, Niu L, Feng B, Kong W, Ren X, Huang F, *et al*: Hypoxia inducible factor-1α drives cancer resistance to cuproptosis. Cancer Cell 43: 937-954.e9, 2025.
45. Zheng J, Li B, Wu Y, Wu X and Wang Y: Targeting arginine methyltransferase PRMT5 for cancer therapy: Updated progress and novel strategies. J Med Chem 66: 8407-8427, 2023.
46. Sun Y, Jin X, Meng J, Guo F, Chen T, Zhao X, Wu H and Ren D: MST2 methylation by PRMT5 inhibits Hippo signaling and promotes pancreatic cancer progression. EMBO J 42: e114558, 2023.
47. Wang Y, Liu X, Zhou L, Duong D, Bhuripanyo K, Zhao B, Zhou H, Liu R, Bi Y, Kiyokawa H and Yin J: Identifying the ubiquitination targets of E6AP by orthogonal ubiquitin transfer. Nat Commun 8: 2232, 2017.
48. Hou A, Xu X, Zhang Y, He H, Feng Y, Fan W, Tan R, Gong L and Chen J: Excessive fatty acids activate PRMT5/MDM2/Drosha pathway to regulate miRNA biogenesis and lipid metabolism. Liver Int 44: 1634-1650, 2024.
49. Cheng J, Bin X and Tang Z: Cullin-RING ligase 4 in cancer: Structure, functions, and mechanisms. Biochim Biophys Acta Rev Cancer 1879: 189169, 2024.
50. Pinner KD, Wales CT, Gristock RA, Vo HT, So N and Jacobs AT: Flavokawains A and B from kava (*Piper methysticum*) activate heat shock and antioxidant responses and protect against hydrogen peroxide-induced cell death in HepG2 hepatocytes. Pharm Biol 54: 1503-1512, 2016.
51. Narayanapillai SC, Leitzman P, O'Sullivan MG and Xing C: Flavokawains A and B in Kava, Not Dihydromethysticin, Potentiate Acetaminophen-Induced Hepatotoxicity in C57BL/6 Mice. Chem Res Toxicol 27: 1871-1876, 2014.
52. Wang Y, Su C, Zhang B, Niu Y, Ren R, Zhao X, Yang L, Zhang W and Ma X: Biological activity, hepatotoxicity, and Structure-activity relationship of kavalactones and flavokavins, the two main bioactive components in kava (*Piper methysticum*). Evid Based Complement Alternat Med 2021: 6851798, 2021.